Rotational spectrum of SO_3 and theoretical evidence for the formation of sixfold rotational energy-level clusters in its vibrational ground state

Daniel S. Underwood, Sergei N. Yurchenko, Jonathan Tennyson, and Per Jensen

Citation: J. Chem. Phys. **140**, 244316 (2014); doi: 10.1063/1.4882865
View online: https://doi.org/10.1063/1.4882865
View Table of Contents: http://aip.scitation.org/toc/jcp/140/24
Published by the American Institute of Physics

Rotational spectrum of SO_3 and theoretical evidence for the formation of sixfold rotational energy-level clusters in its vibrational ground state

Daniel S. Underwood,[1] Sergei N. Yurchenko,[1,a)] Jonathan Tennyson,[1] and Per Jensen[2]
[1]*Department of Physics and Astronomy, University College London, Gower Street, London WC1E 6BT, United Kingdom*
[2]*Fachbereich C-Physikalische und Theoretische Chemie, Bergische Universität, D-42097 Wuppertal, Germany*

(Received 4 March 2014; accepted 22 May 2014; published online 30 June 2014)

The structure of the purely rotational spectrum of sulphur trioxide $^{32}S^{16}O_3$ is investigated using a new synthetic line list. The list combines line positions from an empirical model with line intensities determined, in the form of Einstein coefficients, from variationally computed ro-vibrational wavefunctions in conjunction with an *ab initio* dipole moment surface. The empirical model providing the line positions involves an effective, Watsonian-type rotational Hamiltonian with literature parameter values resulting from least-squares fittings to observed transition frequencies. The formation of so-called 6-fold rotational energy clusters at high rotational excitation are investigated. The SO_3 molecule is planar at equilibrium and exhibits a unique type of rotational-energy clustering associated with unusual stabilization axes perpendicular to the S–O bonds. This behaviour is characterized theoretically in the J range from 100–250. The wavefunctions for these cluster states are analysed, and the results are compared to those of a classical analysis in terms of the rotational-energy-surface formalism. © *2014 AIP Publishing LLC*. [http://dx.doi.org/10.1063/1.4882865]

I. INTRODUCTION

We have previously reported a room-temperature *ab initio* line list for $^{32}S^{16}O_3$,[1] obtained by computing wavenumbers and intensities for rovibrational transitions in the electronic ground state involving rovibrational states with $J \leq 85$ together with the term values of these states. For these calculations, we used the variational quantum-mechanical method outlined in Sec. II. The calculations were based on a potential energy surface (PES) computed entirely by *ab initio* methods.

We made comparisons with the results of extensive experimental studies of this molecule,[2–8] in which several line positions and relative intensities for a number of bands were recorded at room temperature. The computed spectrum generally represented the observations fairly well, albeit with minor discrepancies in the line positions, reflecting small inaccuracies in the purely *ab initio* PES whose parameter values were not refined in least-squares fittings to experimental wavenumber data. As part of this previous work, we scaled a number of reliable experimental relative intensities to our absolute scale, and included these transitions in the HITRAN 2012 database.[9]

Amongst the calculated transitions the "forbidden" rotational spectrum for this trigonal planar molecule was computed. Induced by centrifugal distortions of bond lengths and angles, these transition lines exhibit an interesting structure. Experimentally, only a handful of microwave lines have been measured.[10] As well as these lines being few in number, no intensity values are available for them. In this paper we aim at investigating the behaviour of the rotating SO_3 molecule from a theoretical perspective.

a)Author to whom correspondence should be addressed. Electronic mail: s.yurchenko@ucl.ac.uk

As well as interpreting the rotational spectrum, we also investigate the phenomenon of near-degenerate energy cluster formation in the highly excited rotational states of SO_3. The analysis of the rotational motion of SO_3 gives us an opportunity to characterize, for the first time, such energy cluster formation for a planar tetratomic molecule containing no hydrogen.

Dorney and Watson[11] were the first to explain the formation of quasi-degenerate energy levels for spherical top molecules using classical arguments followed by a series of works based on the classical description of the clustering phenomena.[12–27] Most of these descriptions involve the motion of the molecule about a "localization" axis at high rotational excitation.[11,15,19,22] The clustering phenomenon was further explored in great detail using a formalism based on the rotational energy surface (RES).[28] In this approach, a RES is introduced to describe the classical rotational energy of the molecule as a function of the classical angular momentum vector, and equivalent, stationary points on this surface, so-called relative equilibria, in particular equivalent maxima directly associated with the patterns of rotational energy clusters. For a molecule with structural symmetry (resulting from identical nuclei arranged symmetrically at equilibrium), the rotational energy clusters are associated with the emergence of symmetrically equivalent localization axes recognizable on the RES. This behaviour provides an example of a quantum system approaching a classical limit with increasing energy. The bifurcation of stationary points is important for formation of rotational energy clusters of some types of molecules.[26,29] Zhilinskiĭ[25] also studied the role of symmetry in the cluster formation process in great detail. Usually a RES is obtained from an effective rotational Hamiltonian,[28] which is effectively a perturbation theory expansion. Here we follow a

physically more sound approach where the classical limit is applied to the actual ro-vibrational Hamiltonian (see, for example, Refs. 26, 30, and 31) with the vibrational coordinates optimized by minimizing the classical energy at each orientation of the rotation of the molecule in question.

Typical molecules exhibiting rotational energy clusters are of the type XY_N with a heavy central atom X, Y being H or D, and the X-Y_i bonds being nearly orthogonal,[32,33] which are often referred to as local mode molecules.[32,33] The formation of rotational or ro-vibrational energy-level clusters of this type of molecules was studied for triatomic XH_2 molecules (see, for example, Refs. 22 and 32–35, pyramidal XH_3 molecules, including PH_3,[26,31,33,36] BiH_3, SbH_3,[37] and their deuterated isotopologues.[38] Molecules with heavier Y-atoms can also form rotational energy clusters. The existence of the clustering was predicted for the molecules CF_4,[39–41] SF_6,[12–14] P_4,[24] and experimentally confirmed for SF_6.[42]

For PH_3, BiH_3, and SbH_3, the energy cluster formation was (theoretically) investigated for $J \leq 70$. SO_3 is not a local mode molecule,[32,33] but, as we will show, for SO_3 a pattern of energy clusters is predicted in the present work. However, the clustering behaviour does not manifest itself until the rotational excitation reaches the J range between 100 and 250. SO_3 is also much heavier than the XH_3 molecules, it has much smaller rotational energy spacings and, in consequence, states with much higher J values will be populated at a given temperature. This makes the clustering states of SO_3 potentially accessible experimentally at temperatures of a few hundred °C. Another potential opportunity to reach the required rotational excitations is the rotational centrifuge technique, which allows one to climb the rotational ladder up to the dissociation limit.[43]

The present work deals with two aspects of the SO_3 rotational motion. First, we compute rovibrational energies and wavefunctions using a basis set of high quality in order to simulate accurately the room-temperature microwave (rotational) spectrum and analyse its structure. In this manner, we have calculated rovibrational wavefunctions for $J \leq 85$; this is shown to be adequate for simulating the spectrum at $T = 298.15$ K. The computed wavefunctions are used in conjunction with an *ab initio* dipole moment surface[1] to obtain the room-temperature absorption intensities. These intensities were then combined with line positions obtained from an effective, Watsonian-type rotational Hamiltonian, whose parameter values have been determined in least-squares fittings to experimentally observed transition frequencies.[2–8] This is expected to produce an accurate rotational line list for SO_3, which we recommend for inclusion in the HITRAN[9] and other spectroscopic databases.[44,45] Second, we describe for the first time, both classically and quantum-mechanically, the formation of rotational energy level clusters for a planar $\mathcal{D}_{3h}$(M)-type molecule SO_3.

II. COMPUTATIONAL DETAILS

In computing rovibrational energy levels for SO_3 the TROVE procedure is used, for which the computational details are described extensively elsewhere.[46–49] This procedure was also used to compute our previously published *ab initio* SO_3 line list.[1] Here we reiterate only a few essential details.

The rovibrational Schrödinger equation is solved variationally by diagonalizing a matrix representation of the appropriate Hamiltonian. The Hamiltonian is initially constructed as an expansion of kinetic energy and potential energy operators in terms of suitable linearized coordinates ξ_i^ℓ ($i = 1, \ldots, 5$); the expansion is made around a non-rigid reference configuration as defined by the sixth coordinate ρ. Thus three stretching coordinates, two asymmetric bending coordinates and one out-of-plane-bending coordinate (where the motion described by this latter coordinate is the SO_3 counterpart of the "umbrella-flipping" inversion motion in pyramidal molecules such as NH_3) used to describe the internal motion of SO_3:

$$\xi_k^\ell = 1 - \exp\left(-a\left(r_k^\ell - r_e\right)\right), \quad k = 1, 2, 3, \tag{1}$$

$$\xi_{4a}^\ell = \frac{1}{\sqrt{6}}\left(2\alpha_1^\ell - \alpha_2^\ell - \alpha_3^\ell\right), \tag{2}$$

$$\xi_{4b}^\ell = \frac{1}{\sqrt{2}}\left(\alpha_2^\ell - \alpha_3^\ell\right), \tag{3}$$

$$\sin\bar{\rho} = \frac{2}{\sqrt{3}}\sin[(\alpha_1 + \alpha_2 + \alpha_3)/6], \tag{4}$$

where r_i^ℓ ($i = 1, 2, 3$) and α_k^ℓ ($k = 1, 2, 3$) are linearized versions of the geometrically defined coordinates r_i and α_k[50] with r_i as the bond lengths and α_k as the inter-bond angles. The kinetic energy operator is expanded numerically around the non-rigid reference configuration; for SO_3 this configuration follows the out-of-plane bending motion. When the molecular geometry has $\mathcal{C}_{3v}$ geometrical symmetry,[50,51] ρ is the angle between the C_3 axis and any one of the S–O bonds.

The potential energy expansion used in the TROVE calculation results from transforming a pre-calculated, analytical PES, normally expressed in terms of geometrically defined coordinates such as bond lengths and inter-bond angles, to an expansion in the linearized coordinates $1 - \exp(-a\xi_i^\ell)$ ($i = 1, 2, 3$) and ξ_4^ℓ, ξ_5^ℓ with $a = 2.4$ Å^{-1}. For SO_3, the "original" PES was calculated *ab initio* at the CCSD(T)-F12b level of theory.[1] Once expanded, the Hamiltonian takes the following general form:[47]

$$H = \frac{1}{2}\sum_{\alpha\beta} J_\alpha G_{\alpha\beta} J_\beta + \frac{1}{2}\sum_{\alpha\lambda}\left(p_\lambda G_{\lambda\alpha} + G_{\lambda\alpha} p_\lambda\right)J_\alpha + \frac{1}{2}\sum_{\lambda\nu} p_\lambda G_{\lambda\nu} p_\nu + V + U. \tag{5}$$

Here, J_α ($\alpha = x, y, z$) are rotational momentum operators and p_λ are vibrational momenta conjugate to the coordinates previously defined. The G-values are kinetic energy factors computed numerically as part of the TROVE kinetic energy expansion.[46] V and U are the molecular potential energy function and the pseudopotential resulting from the conversion of the expression for the classical energy to operator form, respectively.

The expansions of the kinetic energy operator and potential energy functions are truncated after the 6th and 8th

order terms, respectively. In order to construct a matrix representation of the Hamiltonian, matrix elements must be computed in terms of a suitable set of basis functions. We define "primitive" sets of 1D basis functions, ϕ_{n_i}, where each set is associated with one of the vibrational coordinates ξ_i^ℓ or ρ; these functions are numerical solutions of 1D Schrödinger equations.[47] The stretching and out-of-plane-bending basis functions are obtained in the Numerov-Cooley approach,[52,53] while harmonic-oscillator eigenfunctions are used as in-plane bending basis functions ϕ_{n_4} and ϕ_{n_5}. These primitive vibrational basis functions are then improved in a two-step contraction scheme,[48] including a solution of the $J = 0$ problem. Subsequently, the eigenfunctions of the $J = 0$ Hamiltonian are used to construct the rovibrational basis functions for $J > 0$; the $J = 0$ basis functions are combined with rigid rotor functions $|J, K, \tau_{\rm rot}\rangle$, where $K = 0, \ldots, J$ and $\tau_{\rm rot}$ determines the rotational parity (see Ref. 54) within the so-called $J = 0$ contraction scheme:[48]

$$\Phi^{(J)}_{\lambda,K,\tau_{\rm rot}} = |J, K, \tau_{\rm rot}\rangle\, \phi^{(J=0)}_{\lambda}, \tag{6}$$

where $\phi^{(J=0)}_{\lambda}$ is a (vibrational) eigenfunction of the $J = 0$ Hamiltonian and λ is a running number identifying the function. The functions $\Phi^{(J)}_{\lambda,K,\tau_{\rm rot}}$ are then symmetrized; each of them generates an irreducible representation of the $\mathcal{D}_{3h}$(M) molecular symmetry group and the function is labelled by this irreducible representation. The symmetrization facilitates the calculation since it factorizes the Hamiltonian matrix into independent symmetry blocks, and this leads to significant savings of computer resources in the diagonalization step. It is important to note that due to the nuclear spin statistics of $^{32}S^{16}O_3$, which is made up entirely of zero-spin bosons, only states of A_1' or A_1'' rovibrational symmetry in $\mathcal{D}_{3h}$(M) exist in nature. Thus, in order to simulate spectra of $^{32}S^{16}O_3$ we need only to compute the rovibrational eigenfunctions that transform accordingly. However, since the rovibrational Hamiltonian for any $J \geq 0$ employs the vibrational ($J = 0$) eigenfunctions, it is advantageous to pre-calculate the $J = 0$ matrix elements for all purely vibrational terms in Eq. (5).

Even though we can discard rovibrational states of $\mathcal{D}_{3h}$(M) symmetries A_2', A_2'', E', and E'', the calculation of the cluster-state wavefunctions and energies for SO_3 is a formidable numerical problem owing to the high J-values, and the associated large ranges of K-values, that we must necessarily consider. This makes severe demands on the computational resources necessary for theoretically computing the associated rovibrational energies, and therefore we reduce the accuracy of the energy calculations in a trade-off between numerical accuracy and computational expense. Our aim is to describe this cluster phenomenon qualitatively and the lack of extreme accuracy is no real problem. To this end we truncate the original basis set using the polyad number

$$P = 2(n_1 + n_2 + n_3) + n_4 + n_5 + \frac{n_6}{2}, \tag{7}$$

which limits the size of the $J = 0$ matrix, and therefore matrices for $J > 0$. The n_i are the principal quantum numbers associated with the 1D basis functions, ϕ_{n_i}, and so they define the number of excited quanta for each vibrational mode considered and can be directly mapped onto the normal-mode quantum numbers traditionally used for labelling vibrational states.[48] In setting up the matrix representations of the rovibrational Hamiltonian in the final step of the calculation, we use only basis functions for which $P \leq P_{\rm max}$. For the current work we use polyad numbers $P_{\rm max}$ of 12 for intensity calculations and $P_{\rm max} = 8$ to investigate the rotational clustering effect. The latter, relatively low $P_{\rm max}$-value is adequate for obtaining a satisfactory description of the energy-cluster formation. A similar approach was taken for the studies of PH_3, BiH_3, and SbH_3.[26,31,36]

III. THE THEORETICAL MICROWAVE SPECTRUM

Figure 1 shows the simulated microwave spectrum for $^{32}S^{16}O_3$, computed with TROVE at $T = 298.15$ K. The spectrum consists of 3 439 transitions between all rotational states with $J \leq 85$. The transitions are subject to the selection rules $\Delta J = J' - J'' = 0, \pm 1$ ($J'' + J' \geq 1$), and symmetry selection rules $A_1' \leftrightarrow A_1''$. The intensity of a transition between two states is given by

$$I(f \leftarrow i) = \frac{8\pi^3 N_A \nu_{if}}{(4\pi\epsilon_0)3hc}\, \frac{e^{-E_i/kT}}{Q(T)} \left[1 - \exp\left(\frac{-hc\nu_{if}}{kT}\right)\right] \times S(f \leftarrow i), \tag{8}$$

where $I(f \leftarrow i)$ is the transition intensity for a transition from state i with energy E_i to state f with energy E_f, with $hc\nu_{if} = E_f - E_i$. Q is the partition function. $S(f \leftarrow i)$ is the line strength, which is defined by the following expression[50] (see also Ref. 46):

$$S(f \leftarrow i) = g_{\rm ns} \sum_{m_f, m_i} \sum_{A=X,Y,Z} \left|\left\langle \Psi^{(\rm f)}_{\rm rv} \middle| \mu_A \middle| \Psi^{(\rm i)}_{\rm rv} \right\rangle\right|^2, \tag{9}$$

with $\Psi^{(\rm i)}_{\rm rv}$ and $\Psi^{(\rm f)}_{\rm rv}$, respectively, as the wavefunctions of the initial and final states i and f, $g_{\rm ns}$ as the nuclear spin statistical weight factor, and μ_A as the electronically averaged component of the molecular dipole moment along the space-fixed axis $A = X, Y, Z$. The sum also runs over the quantum numbers m_i and m_f which are projections (in units of $\hbar$) of the total angular momentum vector $\mathbf{J}$ onto the laboratory-fixed Z axis for the initial and final states, respectively.

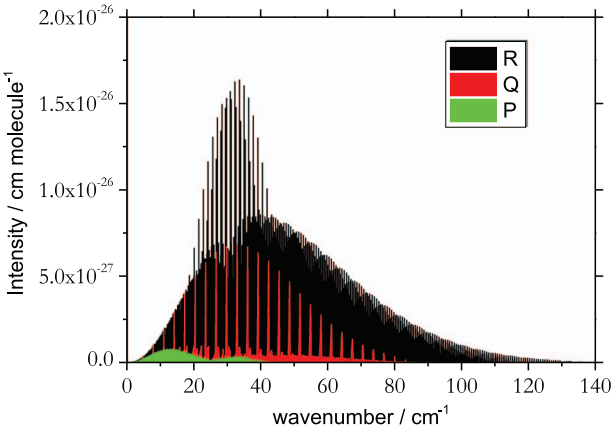

FIG. 1. The microwave spectrum of $^{32}S^{16}O_3$, simulated theoretically at $T = 298.15$ K. Transitions between states with $J \leq 85$ are included; they are color-coded in the diagram to indicate the various transition types.

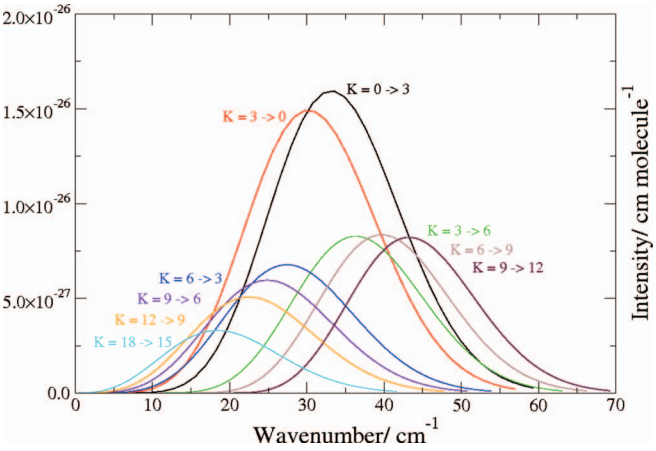

FIG. 2. The strongest individual K sub-bands of the R-branch in the purely rotational spectrum of $^{32}S^{16}O_3$.

The color coding in Fig. 1 distinguishes the P-, Q-, and R-branches in the spectrum. We see that in each branch, the intensities depend on J in a characteristic manner. Figure 2 expands the wavenumber scale for the R-branch and the structures of the individual K sub-bands are indicated. The intensities of the K sub-bands decrease gradually as the K-values involved increase. SO_3 has $\mathcal{D}_{3h}$ symmetry at equilibrium and, in consequence, no "permanent" dipole moment. Therefore, the transitions in Figure 1 are "forbidden," that is, they are induced by the rotation-vibration interaction as explained, for example, in Sec. 14.1.14 of Ref. 50. The transitions satisfy the selection rules $A_1' \leftrightarrow A_1''$ mentioned above and states of rovibrational symmetry A_1' or A_1'' occur when the value of the quantum number K (which is not a "good," rigorously defined quantum number, but which can nevertheless be conveniently used for labelling the SO_3 rotational energies) is a multiple of 3: $K = 0, 3, 6, \ldots$. Figure 2 shows that the strongest sub-bands have $K = 0 \leftarrow 3$ and $K = 3 \leftarrow 0$. In general, strong sub-bands satisfy $\Delta K = \pm 3$ and the band intensity decreases as $K \rightarrow J$.

Analysing the wavefunctions we find that each wavefunction $\Psi_n^{(J,\Gamma)}$ has dominant contributions from the $\Phi_\lambda^{(J=0,A_1')}$ basis functions with $\lambda = 1$ and thus associated with the vibrational ground state. However, there are other significant contributions associated with the ν_2 and ν_4 bending vibrational modes, respectively. Thus, even in the vibrational state conventionally labelled as the ground state, there is a non-negligible probability of finding the molecule with the ν_2 or ν_4 vibrational mode excited by one quantum.

The contributions to the eigenfunctions from the ν_2 and ν_4 basis states are highest at $K = 0$ and drop as $K \rightarrow J$. We can straightforwardly explain this classically. For a given J-value, the rotational eigenstates of SO_3 that we conventionally label by $K = J$ and $K = 0$ correspond to the two limiting cases of the molecule rotating about the z-axis (which, in configurations of $\mathcal{C}_{3v}$ geometrical symmetry, coincides with the C_3 symmetry axis) and about axes perpendicular to the z axis, respectively. A rotation about the z axis preserves the high $\mathcal{D}_{3h}$(M) geometrical symmetry that the molecule has at equilibrium and the dipole moment vanishes at $\mathcal{D}_{3h}$(M)-symmetry configurations, also for $K \rightarrow J$. For $K = 0$, the situation is quite different. The angular momentum vector of length $\sqrt{J(J+1)}\hbar$ now results from rotation about axes perpendicular to the z axis and this, in turn, gives rise to centrifugal forces that deform the molecule away from $\mathcal{D}_{3h}$(M) geometrical symmetry, leading to the formation of a small, non-vanishing dipole moment in the vibrational ground state (see also the prediction of a pure rotational spectrum of H_3^+[55,56]). This explains the form of the rotational band in Fig. 1: the strongest transitions involve the states with the smallest K-values. The transitions in the two bands with $K = 0 \leftarrow 3$ and $K = 3 \leftarrow 0$, respectively, have intensities (and Einstein coefficients) about twice as strong as the transitions in the bands involving states with $K \neq 0$ only. Quantum mechanically, this is explained by the special-case nature of the $K = 0$ wavefunctions giving rise to an "extraneous" factor of 2 in the expression for the line strength (see, for example, Eq. (12.33) of Ref. 51). A more detailed analysis of the rotational eigenfunctions obtained at very high J-values is presented below in connection with the discussion of the rotational-cluster-formation phenomenon.

IV. A HYBRID, EMPIRICAL-*AB INITIO* ROTATIONAL LINE LIST FOR $^{32}S^{16}O_3$

We have previously generated a list of transitions for $^{32}S^{16}O_3$ which were included in the 2012 edition of the HITRAN database.[9] For this we took available experimental transitions[2–8] and compared this experimental data to entries in our computed room-temperature line list, adapting the relative intensity measurements to our absolute scale.[1] At the same time, we also presented a variationally computed, *ab initio* line list for $^{32}S^{16}O_3$. In this list, both the line positions and the transition intensities were obtained variationally with TROVE. However, the line positions of 25 pure rotational transitions were measured by Meyer *et al.*[10] and our HITRAN line list included these 25 experimental microwave lines augmented with our theoretical values for the transition intensities. In the present work, we extend our room-temperature line list to include additional rotational transitions. For this we use the ground state rotational constants and centrifugal distortion parameters for $^{32}S^{16}O_3$ of Maki *et al.*[5] in conjunction with the expression

$$\begin{aligned} F(J,K) &= B_0 J(J+1) + (C_0 - B_0)K^2 - D_0^J [J(J+1)]^2 \\ &\quad - D_0^{JK} J(J+1)K^2 - D_0^K K^4 + H_0^J [J(J+1)]^3 \\ &\quad + H_0^{JK} [J(J+1)]^2 K^2 + H_0^{KJ} J(J+1)K^4 \\ &\quad + H_0^K K^6 \pm \delta_{3K} \Delta_0 [J(J+1)][J(J+1)-2][J(J+1)-6] \end{aligned} \tag{10}$$

to generate rotational energies for J up to 85. These constants have already been used in the analysis of the spectra presented in Refs. 2–8. To make sure that the extrapolation to high-J states is reasonable, we compare the energy values determined from Eq. (10), and the corresponding transition wavenumbers, with those generated by TROVE. We find a very good agreement, with a root-mean-square difference of only 0.0167 cm^{-1} for all rotational transitions involving states with

TABLE I. Comparison of rotational term values for $^{32}S^{16}O_3$ obtained by inserting the experimentally derived, effective rotational constant values from Maki *et al.*[5] in Eq. (10) ("Obs.") with theoretical TROVE values from the present work ("Calc.").

J	K	Obs. (cm^{-1})	Calc. (cm^{-1})
5	3	8.885	8.886
10	9	24.200	24.203
10	0	38.336	38.342
20	18	89.825	89.837
20	0	146.333	146.355
50	48	486.469	486.514
50	0	886.775	886.897
85	84	1315.569	1315.283
85	3	2529.972	2530.258

$J \leq 85$. Table I shows examples of comparisons between rotational term values in the vibrational ground state of $^{32}S^{16}O_3$ calculated from Eq. (10) and values obtained variationally with TROVE. The 25 lines from the previous HITRAN-suitable list were taken from Meyer *et al.*[10] These transitions are replicated by Eq. (10) to within the precision quoted in our updated list. We expect that the values from Eq. (10) are more accurate than the TROVE values, so use these line positions and combine them absorption intensities (Einstein coefficients) determined from the *ab initio* dipole moment surface. We suggest that these new 3 414 transitions for $^{32}S^{16}O_3$ be added to HITRAN and other spectroscopic databases; they constitute a significant extension on the 25 microwave transitions presently included in HITRAN.

V. ROTATIONAL ENERGY CLUSTER FORMATION IN HIGH-*J* STATES OF SO_3

To investigate the possible rotational-energy cluster formation in SO_3, we have computed rovibrational term values of $^{32}S^{16}O_3$ for $J \leq 250$. The present work is focused on rovibrational states in the vibrational ground state, and so the calculation aims at obtaining accurate results for these states only. Because of this, we were able to reduce with impunity the size of the vibrational basis: We employ only basis functions satisfying $P \leq P_{\max} = 8$ (see Sec. II). We denote a rotational term value for SO_3 as $E_{J,K}$ and define the reduced energy $\Delta E_{J,K} = E_{J,K} - E^{\max}_{J,K}$, where $E^{\max}_{J,K}$ is the maximum energy found in a given J multiplet of the vibrational ground state (see, for example, Refs. 26, 31, 36, and 37). We visualize the rotational-energy-cluster formation by plotting the reduced energies $\Delta E_{J,K}$ against J in Fig. 3(a) for all states including those forbidden by the nuclear state statistics. The figure shows that for $J > 150$, energy-level clusters form for $^{32}S^{16}O_3$ in a manner similar to that previously described for the pyramidal molecules PH_3, BiH_3, and SbH_3[26,31,36,37] at significantly lower J values. The four highest energies in each J manifold cluster together. In conventional symmetric-top notation, these highest four energy levels, taken in descending order, have $K = |k| = 0$, 1, 2, and 3, respectively, and the $\mathcal{D}_{3h}$(M) symmetries A_1', E'', E', and A_2'' (A_2', E'', E', and A_1'') for J even (odd). Since the states of E symmetry are doubly degenerate, the four energies define a near-degenerate six-fold cluster. However, for $S^{16}O_3$, only one of these four levels is symmetry allowed by the nuclear statistics, see Fig. 3(a), where these levels are indicated with crosses; for other isotopologues, e.g., $S^{18}O_3$, all of the levels exist.

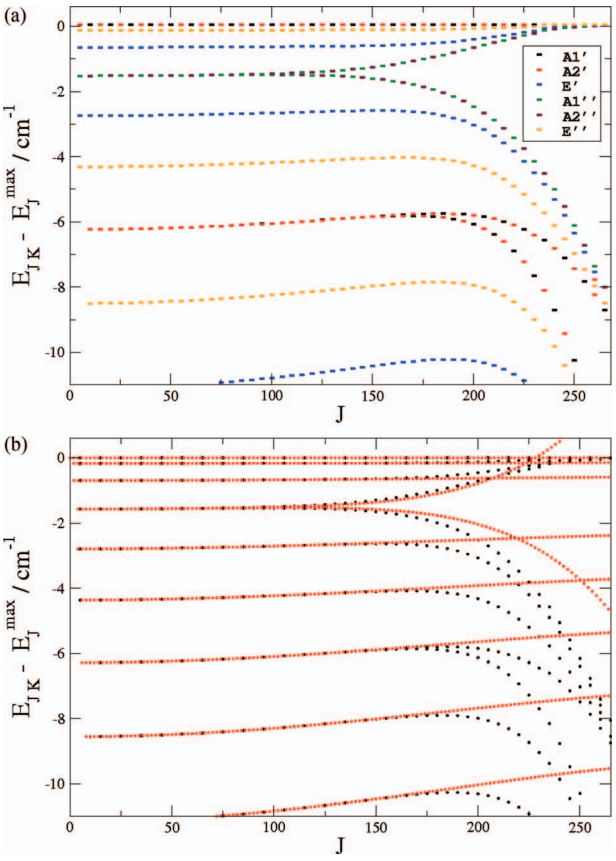

FIG. 3. (a) Reduced energies $\Delta E_{J,K}$ plotted against J for $^{32}S^{16}O_3$. The $\Delta E_{J,K}$-values are calculated with TROVE. The symmetry of the $E_{J,K}$ levels is indicated by color. We note that only A_1' (black) and A_1'' (green) are allowed by Bose-Einstein statistics. (b) Reduced energies $\Delta E_{J,K}$ plotted against J for $^{32}S^{16}O_3$. Reduced energy values obtained with TROVE (black) are compared to experimentally derived values (red) from Ref. 5.

Figure 3(b) compares the reduced energy values obtained with TROVE with values determined from Eq. (10), using the experimentally derived values of the required rotation-vibration parameters from Ref. 5. Although the reduced energies obtained from Maki *et al.* Equation (10) does not exhibit a 6-fold cluster formation at the high J limit, there is a clear tendency in the shape of the $K = 3$ curve to approach the topmost, $K = 0$ energy levels. However, all other rotational states are completely misplaced indicating the deficiency of the simplistic model of Eq. (10) to describe the energy levels with very high J. The expansion (10) is truncated after the 6th order terms and we must expect that higher-order terms become important at $J > 150$. In consequence, Eq. (10) is not suitable for extrapolation to states with so high J-values, and we take the TROVE results to be more reliable.

A. Origin of the cluster states

It is accepted and has been described in detail[25] that rotational clustering is associated with symmetry breaking of

the RES and the corresponding stationary points. For the XY_3 type pyramidal molecules the formation of six-fold rotational-energy clusters can be explained in terms of classical arguments that we outline briefly here. In the cluster states, the rotation of XY_3 can be thought of as taking place around one of three possible, so-called localization axes, which represent the stationary points, or relative equilibria of the corresponding RES.[26,31,37] For pyramidal XY_3 molecules these three symmetrically equivalent axes are of the C_2 type and nearly coincide with the three X-H_i bonds of the XH_3 molecule, where H_i is the proton labelled $i = 1$, 2, or 3.[31,37] For each of the three localization axes there is the possibility of clockwise or anticlockwise rotation and so six equivalent physical situations emerge, all six having approximately the same energy. The stationary points are the six maxima on the RES,[26] which constitute a six-fold near-degenerate energy cluster. The cluster states are stabilized by large energy barriers separating each of the six equivalent situations just described.

Quantum mechanically of the concept a *primitive cluster state* (PCS) function is customarily used to describe these situations.[30–32] When the PCSs are separated by energy barriers so high as to effectively prevent tunneling between the states, the six equivalent PCS situations become degenerate and the manifold of wavefunctions associated with their common energy can be viewed as a six-dimensional space where the PCS, or coherent wavefunctions, serve as a convenient basis set. Jensen and Kozin[30] constructed the PCS wavefunctions of an XH_2 molecule using the symmetry properties of the corresponding eigenstates. Yurchenko *et al.*[31] obtained the PCS wavefunctions for an XH_3 molecule by diagonalizing a matrix representing the angular momentum. Below we follow this latter approach in constructing and visualizing the (quantum-mechanical) PCS wavefunctions for SO_3, a planar XY_3 molecule.

B. Classical analysis in terms of the rotational energy surface

Classically, the rotational cluster formation can be understood in terms of the topology of the rotational energy surface. For a given value of J, the RES is obtained as a radial plot of the function $E_J(\theta, \phi)$. This function yields the classical rotational energy in terms of the two angles (θ, ϕ) defining the orientation of the classical angular momentum vector in the molecule-fixed axis system xyz. Thus, the xyz components of the classical angular momentum vector, (J_x, J_y, J_z), are given by according to the relations

$$J_x = \sqrt{J(J+1)}\hbar \sin\theta \cos\phi, \tag{11}$$

$$J_y = \sqrt{J(J+1)}\hbar \sin\theta \sin\phi, \tag{12}$$

$$J_z = \sqrt{J(J+1)}\hbar \cos\theta, \tag{13}$$

where $\theta \in [0, \pi]$ and $\phi \in [0, 2\pi]$. Obviously, in this semiclassical approach we assume the angular momentum vector to have its "quantum-mechanical" length of $\sqrt{J(J+1)}\hbar$.

A traditional approach to construct RES is to apply Eqs. (11)–(13) to an effective rotational Hamiltonian.[11,16,18,20,57] We follow and alternative, perturbation-theory free approach[26,30,31] and obtain a classical Hamiltonian function $H_{\rm rv}$ by applying the classical limit to the quantum-mechanical Hamiltonian operator $\hat{H}$ (Eq. (5)), i.e., to an "*ab initio* Hamiltonian" as was proposed by Harter.[18] Here, $\hat{T}$ is the classical kinetic energy and the momentum p_n (n= 1, 2, …, 6) are conjugate to the generalized coordinates ξ_n^ℓ and ρ described above. The rotational energy surface $E_J(\theta, \phi)$ is then generated on a regular grid of angle points θ_m, ϕ_m by setting the vibrational coordinates in $\hat{H}$ to the optimized geometries $\xi_n^{(\rm opt)}$ and $\rho^{(\rm opt)}$ for each orientation of the angular momentum defined by the polar and azimuthal angles (θ_m, ϕ_m) and Eqs. (11)–(13):

$$E_J(\theta_m, \phi_m) = H_{\rm rv}\left(J, \xi_n^\ell = \xi_n^{(\rm opt)}, \rho = \rho^{(\rm opt)}; \theta_m, \phi_m\right). \tag{14}$$

We also set the generalized vibrational momenta $p_n = \partial T/\partial \dot{q}_n$ to zero,[22] which has been shown to be a good approximation.[31,36] A more accurate approach[26] is to include the values of classical p_n into the optimization procedure. Finally, the RES is given by a radial plot of the function

$$E_J^{(\rm RES)}(\theta_m, \phi_m) = E_J(\theta_m, \phi_m) - E_J^{(\rm min)}, \tag{15}$$

where $E_J^{(\rm min)}$ is the minimum value of $E_J(\theta_m, \phi_m)$. An example of the RES of SO_3, computed for $J = 200$, is shown in Fig. 4. The resulting RES has a doughnut-like shape with six symmetrically equivalent maxima in the xy plane (i.e., for $\theta = 90^\circ$). These maxima are difficult to recognize in Fig. 4 but they are better seen in the top display of Fig. 5, which shows the slice of the RES along a path where θ_m is kept constant at 90° and ϕ_m is varied from 0°–360°.

We have already mentioned that when energy clusters form for pyramidal XH_3 molecules, the six maxima on the RES corresponding to the top clusters in a J manifold are located in the directions defined by the local C_2 symmetry axes associated with the plane containing a X–H molecular bond. For SO_3, however, the six maxima appear for $\theta = 90^\circ$ and $\phi = 30^\circ$, 90°, 150°, 210°, and 330°, respectively, all in the molecular plane. Each of these directions is perpendicular to one of the S–O bonds and also define the orientations of the localization axes A. The molecular geometries corresponding to the maxima on the RES are illustrated by the two lower panels of Fig. 5. For a molecular geometry, associated with the first stationary rotational axis and illustrated in Fig. 6, the localization axis $A = C_2'$ is perpendicular to the S–O_1 bond and the molecular structure has a $\mathcal{C}_{2v}$(M) symmetry with

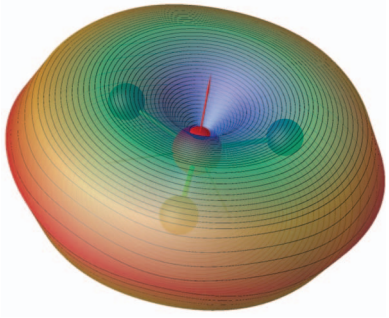

FIG. 4. The rotational energy surface of SO_3 at $J = 200$.

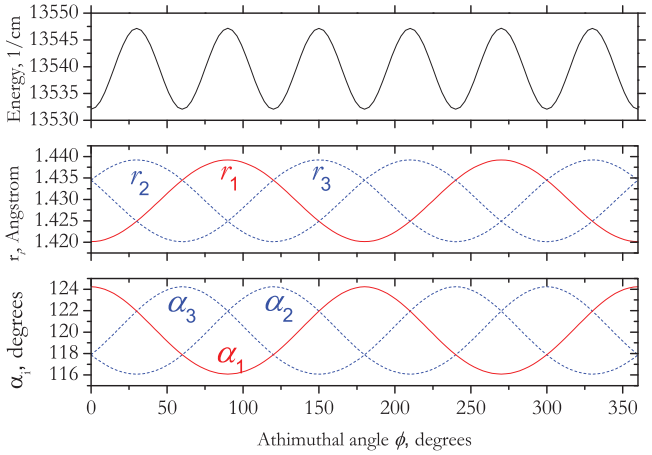

FIG. 5. Top display: A 1D cut through the $J = 200$ RES of SO_3 for $\theta = 90°$ and $\phi \in [0°, 360°]$. Middle display: The ϕ-dependence (at $\theta = 90°$) of the vibrationally averaged values for the three bond lengths r_1, r_2, r_3. Bottom display: The ϕ-dependence (at $\theta = 90°$) of the vibrationally averaged values for the three inter-bond angles $\alpha_1 = \angle(O_2–S–O_3)$, $\alpha_2 = \angle(O_1–S–O_3)$, and $\alpha_3 = \angle(O_1–S–O_2)$.

S–O_2 and S–O_3 elongated and the angle $\alpha_1 = \angle(O_2–S–O_3)$ reduced from 120° to 112.4°. These six maxima are relatively small and separated by less pronounced barriers comparing to the clustering of XH_3 pyramidal molecules. However, their rotational energy-clustering structure (see Fig. 3) is very similar, despite these differences in the topology of the RESs of a planar SO_3 molecule from that encountered for pyramidal XY_3 molecules.

C. Quantum-mechanical analysis

We supplement the classical RES analysis of the cluster-formation phenomenon by a determination of the quantum-mechanical PCS wavefunctions; these wavefunctions are obtained using a technique already described elsewhere.[31,32] For a given J-value, we solve the Schrödinger equation for the Hamiltonian in Eq. (5) using TROVE. That is, we initially diagonalize the Hamiltonian matrix blocks for all $\mathcal{D}_{3h}(M)$ symmetries, using the basis set defined by $P_{max} = 8$. We then select the six near-degenerate eigenfunctions $\psi_n^{(J)}$ associated with the "top" cluster in the appropriate J manifold of the vibrational ground state, and search for six localization directions A_i and associated $|i\,\mathrm{PCS}\rangle$ as linear combinations of $\psi_n^{(J)}$ such that the molecule has the largest possible absolute value of the angular momentum projection, $J\hbar$, onto the localization axis A_i associated with $|i\,\mathrm{PCS}\rangle$. This procedure is justified when the six states $\psi_n^{(J)}$ are so close to being degenerate that any linear combination of them can be taken to be an eigenfunction of the rovibrational Hamiltonian. For example, in the two states $|1\,\mathrm{PCS}\rangle$ and $|2\,\mathrm{PCS}\rangle$, the molecule has angular momentum projections of $+m\hbar$ and $-m\hbar$, respectively, with $m \approx J$, onto the localization axis A_1. In the case of SO_3 we know that the localization axes are in the molecular plane ($\theta_A = 90°$) and only the azimuthal angle ϕ_A must be determined. In agreement with the classical results, the localization axes are found to be perpendicular to one of the S–O bonds, that is, with $\phi_A = 30°$, 90°, 150°, 210°, 270°, or 330°. It should be noted that the PCS functions associated with these directions could be also obtained from the six eigenfunctions $\psi_n^{(J)}$ based solely on their symmetries, see, for example, Ref. 30.

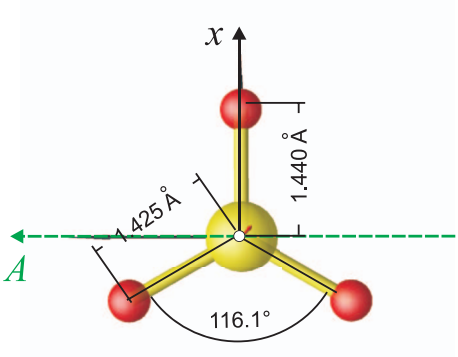

FIG. 6. The schematic representation of the optimized structure of SO_3 at $J = 200$ corresponding to one of the maxima on the RES.

We visualize the PCS states by plotting their reduced rotational densities, obtained by integrating the square of corresponding wavefunction $|n\ \mathrm{PCS}\rangle$ over all vibrational coordinates and over the Euler angle α:

$$F(\beta, \gamma) = \int_0^{2\pi} \mathrm{d}\alpha \int_{\mathrm{vib}} \mathrm{d}V \left(\psi_n^{\mathrm{PCS}}\right)^* \psi_n^{\mathrm{PCS}}, \qquad (16)$$

where $\psi_n^{\mathrm{PCS}} = |n\ \mathrm{PCS}\rangle$ and $\mathrm{d}V$ is the volume element associated with the vibrational coordinates. We use the explicit form of the rotational functions $D_{J,k,m}(\alpha, \beta, \gamma)$[50] for $m = J$ so that the molecule is aligned with the angular momentum oriented along the space fixed Z axis to the greatest extent allowed by quantum mechanics (see Ref. 31 for details). The Euler angles β, γ define the orientation of the space-fixed Z axis relative to the molecule-fixed axis system xyz. Examples of probability distributions $F(\beta, \gamma)$ obtained for $\psi = |1\,\mathrm{PCS}\rangle$ at $J = 100$, 150, 200, and 250 are shown in Fig. 7 (Multimedia view), where the $F(\beta, \gamma)$ functions are imaged onto Bloch spheres of arbitrary radii. The maxima of the $F(\beta, \gamma)$ distributions indicate how the molecule prefers to align itself relative to the space-fixed Z axis and, since $m = J$, to the angular momentum vector which we can think of as being classical in these highly excited rotational states. The classical angular momentum vector is conserved in space and time so that it defines the axis of rotation. The vibrationally averaged structure, the molecule-fixed axis system xyz, and the localization axis A are indicated for the $|1\,\mathrm{PCS}\rangle$ state in Fig. 6. We illustrate how cluster states differ from non-cluster states in Fig. 8 (Multimedia view) which represents the probability distributions $F(\beta, \gamma)$ for the states with $(J, K) = (100, 99)$ and (100, 96), respectively. In these states, the rotation obviously takes place around the z axis which is perpendicular to the molecular plane and the angular momentum precesses about this axis. In the two panels of Fig. 8 (Multimedia view), the precessing angular momentum forms angles of roughly 9° and 18°, respectively, with the z axis. The angles associated with these precessions compare well with the classical interpretation of the orientation of the rotation axis relative to the z axis defined

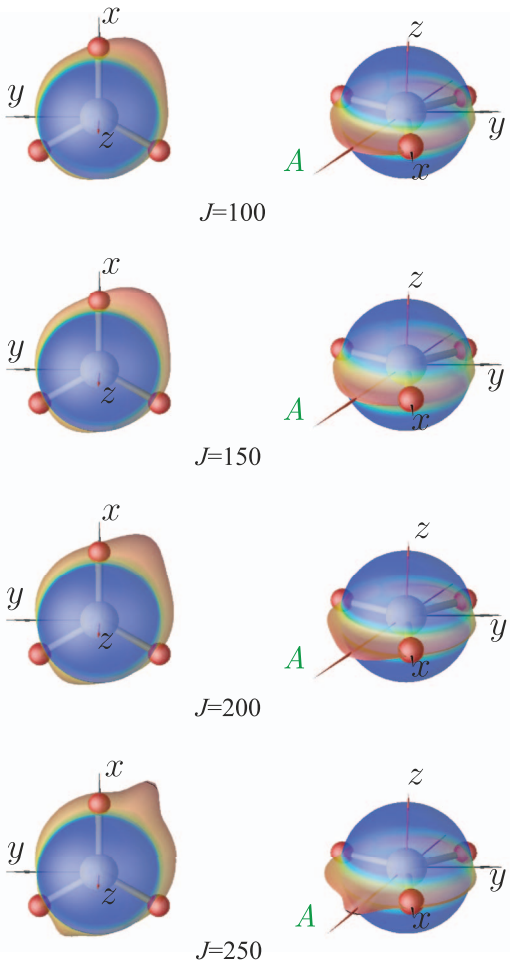

FIG. 7. Probability distribution functions $F(\beta, \gamma)$ obtained for PCS states with $J = 100$, 150, 200, and 250 in the vibrational ground state of $^{32}S^{16}O_3$. (Multimedia view) [URL: http://dx.doi.org/10.1063/1.4882865.1]
[URL: http://dx.doi.org/10.1063/1.4882865.2]
[URL: http://dx.doi.org/10.1063/1.4882865.3]
[URL: http://dx.doi.org/10.1063/1.4882865.4]

as (see, for example, Refs. 16 and 37)

$$\theta_k = \arccos\left(\frac{\pm K_{\rm lc}}{\sqrt{J(J+1)}}\right). \qquad (17)$$

For $K = 99$ and $K = 96$ ($J = 100$) we obtain $\theta_k = 10^\circ$ and 17°, respectively.

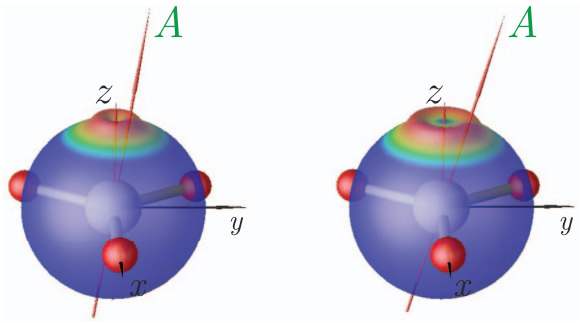

FIG. 8. Probability distribution functions $F(\beta, \gamma)$ for the rotational states with $(J, K) = (100, 99)$ and $(100, 96)$, respectively, in the vibrational ground state of $^{32}S^{16}O_3$. (Multimedia view)
[URL: http://dx.doi.org/10.1063/1.4882865.5]
[URL: http://dx.doi.org/10.1063/1.4882865.6]

VI. SUMMARY AND CONCLUSION

As part of the present work we have generated a "hybrid" line list for $^{32}S^{16}O_3$, consisting of 3 414 rotational transitions in the vibrational ground state. The transitions take place between rotational states with J-values in the range from 0 to 85. The frequencies of the 3 414 rotational transitions are obtained using the "Watsonian" expression of Eq. (10) with the values of the $^{32}S^{16}O_3$ ground state rotational constants obtained by Maki *et al.*[5] by least-squares fits to their observed infrared frequencies. The line list values for the intensities of the rotational transitions are purely theoretical. They are computed with the TROVE program[46–49] from *ab initio* potential energy and dipole moment surfaces reported previously.[1] We suggest that the new line list data be included in the HITRAN database[9] since, at present, the only SO_3 information available there comprises 25 experimentally measured line frequencies for rotational transitions of $^{32}S^{16}O_3$. The new theoretical data from the present work are given as the supplementary material[58] and also available at www.exomol.com as a part of the ExoMol project.[59]

Furthermore, we have investigated in the present work by theoretical methods the formation of near-degenerate rotation-vibration energy clusters in the vibrational ground state of $^{32}S^{16}O_3$ at high rotational excitation. We report here for the first time theoretical predictions of such cluster states for an XY_3 molecule that is planar at equilibrium. Using variational nuclear motion calculations we predict the formation of six-fold near-degenerate energy-level clusters in the vibrational ground state of $^{32}S^{16}O_3$ in the J range between 100 and 250. The structure of the rotational energy clusters is similar to from that previously described for the pyramidal XH_3 molecules. However the cluster-formation mechanism is different: Whereas in the pyramidal molecules the rotation in the cluster states can be thought of as taking place around so-called stabilization axes roughly coinciding with the X–H bonds, for SO_3 each stabilization axis is perpendicular to one of the S–O bonds, see Fig. 6. In the cluster states at $J \geq 100$, the bond perpendicular to the stable rotational axis is significantly elongated by centrifugal forces. Since the two other bonds are not orthogonal to the axis of rotation, they are less elongated, but the angle α_1 between them is decreased by the centrifugal distortion (Fig. 6).

The rotational-energy clustering of SO_3 is special because of the small rotational constants. Since the rotational clustering of heavy molecules, such as CF_4 and SF_6, has been successfully studied experimentally, we hope that our results will encourage experimentalists to confirm the existing stabilization rotations for SO_3 as well. Indeed highly excited rotational levels of SO_3 should be present and observable at temperatures about 800 K using recently proposed techniques.[60] We note once again that for the $S^{16}O_3$ isotopologue, the clusters are hypothetical since in this case, the nuclear statistics permits only rotation-vibration states of A_1' and A_1'' symmetry and so in reality, each six-fold cluster will comprise a single existing energy level accompanied by three "missing levels." For isotopologues containing oxygen isotopes with nonzero spin such as $S^{18}O_3$, however, all cluster components will exist.

Apart from high-T conventional spectroscopy, another possibility of populating highly excited rotational states experimentally is by the optical-centrifuge technique pioneered by Karczmarek *et al.*[43] In Ref. 61, it was speculated for other molecules with energy clusters that states with PCS properties could be prepared by means of optical-centrifuge techniques. These states are given as superpositions of near-degenerate energy eigenstates and would therefore be long-lived. In consequence, it may be possible to verify their existence experimentally. Again, the formation of the PCS-like states cannot take place for $S^{16}O_3$ since the required near-degenerate eigenstates are missing, but for $S^{18}O_3$ such experiments could be feasible.

Finally we note that a hot SO_3 line list is under construction as part of ExoMol project.[59] Results of these calculations will be reported elsewhere.[62]

ACKNOWLEDGMENTS

We thank Alexander Fateev for stimulating our interest in this molecule and for helpful discussions. This work was supported by Grant No. 10442 from energinet.dk under a subcontract from the Danish Technical University and the ERC under Advanced Investigator Project 267219.

[1]D. S. Underwood, J. Tennyson, and S. N. Yurchenko, Phys. Chem. Chem. Phys. **15**, 10118–10125 (2013).
[2]A. Kaldor, A. G. Maki, A. J. Dorney, and I. M. Mills, J. Mol. Spectrosc. **45**, 247–252 (1973).
[3]J. Ortigoso, R. Escribano, and A. G. Maki, J. Mol. Spectrosc. **138**, 602–613 (1989).
[4]E. T. H. Chrysostom, N. Vulpanovici, T. Masiello, J. Barber, J. W. Nibler, A. Weber, A. Maki, and T. A. Blake, J. Mol. Spectrosc. **210**, 233–239 (2001).
[5]A. Maki, T. A. Blake, L. S. Sams, N. Vulpanovici, J. Barber, E. T. H. Chrysostom, T. Masiello, J. W. Nibler, and A. Weber, J. Mol. Spectrosc. **210**, 240–249 (2001).
[6]J. Barber, E. T. H. Chrysostom, T. Masiello, J. W. Nibler, A. Maki, A. Weber, T. A. Blake, and R. L. Sams, J. Mol. Spectrosc. **216**, 105–112 (2002).
[7]S. W. Sharpe, T. A. Blake, R. L. Sams, A. Maki, T. Masiello, J. Barber, N. Vulpanovici, J. W. Nibler, and A. Weber, J. Mol. Spectrosc. **222**, 142–152 (2003).
[8]A. Maki, T. A. Blake, R. L. Sams, J. Frieh, J. Barber, T. Masiello, E. T. H. Chrysostom, J. W. Nibler, and A. Weber, J. Mol. Spectrosc. **225**, 109–122 (2004).
[9]L. S. Rothman, I. E. Gordon, Y. Babikov, A. Barbe, D. C. Benner, P. F. Bernath, M. Birk, L. Bizzocchi, V. Boudon, L. R. Brown, A. Campargue, K. Chance, E. A. Cohen, L. H. Coudert, V. M. Devi, B. J. Drouin, A. Fayt, J.-M. Flaud, R. R. Gamache, J. J. Harrison, J.-M. Hartmann, C. Hill, J. T. Hodges, D. Jacquemart, A. Jolly, J. Lamouroux, R. J. Le Roy, G. Li, D. A. Long, O. M. Lyulin, C. J. Mackie, S. T. Massie, S. Mikhailenko, H. S. P. Müller, O. V. Naumenko, A. V. Nikitin, J. Orphal, V. Perevalov, A. Perrin, E. R. Polovtseva, C. Richard, M. A. H. Smith, E. Starikova, K. Sung, S. Tashkun, J. Tennyson, G. C. Toon, V. G. Tyuterev, and G. Wagner, J. Quantum Spectrosc. Radiat. Transf. **130**, 4–50 (2013).
[10]V. Meyer, D. H. Sutter, and H. Dreizler, Z. Naturforsch. A **46**, 710–714 (1991).
[11]A. J. Dorney and J. K. G. Watson, J. Mol. Spectrosc. **42**, 135 (1972).
[12]W. G. Harter and C. W. Patterson, Int. J. Quantum Chem. **12**, 479–492 (1977).
[13]C. W. Patterson and W. G. Harter, J. Chem. Phys. **66**, 4886–4892 (1977).
[14]W. G. Harter and C. W. Patterson, J. Chem. Phys. **66**, 4872–4885 (1977).
[15]W. G. Harter and C. W. Patterson, Phys. Rev. Lett. **38**, 224–227 (1977).
[16]W. G. Harter and C. W. Patterson, J. Chem. Phys. **80**, 4241–4261 (1984).
[17]B. I. Zhilinskiĭ and I. M. Pavlichenkov, Z. Eksperim. Teor. Fiz. **92**, 387–403 (1987).
[18]W. G. Harter, Comput. Phys. Rep. **8**, 319–394 (1988).
[19]B. I. Zhilinsky and I. M. Pavlichenkov, Opt. Spektrosk. **64**, 688–690 (1988).
[20]D. A. Sadovskiĭ and B. I. Zhilinskiĭ, Mol. Phys. **65**, 109–128 (1988).
[21]D. A. Sadovskiĭ, B. I. Zhilinskiĭ, J. P. Champion, and G. Pierre, J. Chem. Phys. **92**, 1523–1537 (1990).
[22]I. N. Kozin and I. M. Pavlichenkov, J. Chem. Phys. **104**, 4105–4113 (1996).
[23]I. N. Kozin, R. M. Roberts, and J. Tennyson, J. Chem. Phys. **111**, 140–150 (1999).
[24]C. van Hecke, D. A. Sadovskiĭ, B. I. Zhilinskiĭ, and V. Boudon, Eur. Phys. J. D **17**, 13–35 (2001).
[25]B. I. Zhilinskiĭ, Phys. Rep. **341**, 85–171 (2001).
[26]S. Petrov and B. M. Kozlovskii, J. Mol. Spectrosc. **243**, 245–252 (2007).
[27]W. G. Harter and J. C. Mitchell, Int. J. Mol. Sci. **14**, 714–806 (2013).
[28]W. G. Harter, Phys. Rev. A **24**, 192–263 (1981).
[29]I. M. Pavlichenkov and B. I. Zhilinskiĭ, Ann. Phys. **184**, 1–32 (1988).
[30]P. Jensen and I. N. Kozin, J. Mol. Spectrosc. **160**, 39–57 (1993).
[31]S. N. Yurchenko, W. Thiel, S. Patchkovskii, and P. Jensen, Phys. Chem. Chem. Phys. **7**, 573–582 (2005).
[32]P. Jensen, Mol. Phys. **98**, 1253–1285 (2000).
[33]P. Jensen, *Wiley Interdisciplinary Reviews: Computational Molecular Science* (John Wiley & Sons, Inc., 2012), Vol. 2, pp. 494–512.
[34]P. Jensen, G. Osmann, and I. N. Kozin, in *Advanced Series in Physical Chemistry: Vibration-Rotational Spectroscopy and Molecular Dynamics*, edited by D. Papousek (World Scientific Publishing Company, Singapore, 1997), Vol. 9, pp. 298–351.
[35]S. N. Yurchenko, W. Thiel, P. Jensen, and P. R. Bunker, J. Mol. Spectrosc. **239**, 160–173 (2006).
[36]S. N. Yurchenko, M. Carvajal, W. Thiel, and P. Jensen, J. Mol. Spectrosc. **239**, 71–87 (2006).
[37]S. N. Yurchenko, W. Thiel, and P. Jensen, J. Mol. Spectrosc. **240**, 174–187 (2006).
[38]S. N. Yurchenko, R. I. Ovsyannikov, W. Thiel, and P. Jensen, J. Mol. Spectrosc. **256**, 119–127 (2009).
[39]B. I. Zhilinskii, S. Brodersen, and M. Madsen, J. Mol. Spectrosc. **160**, 192–216 (1993).
[40]S. Brodersen and B. I. Zhilinskiĭ, J. Mol. Spectrosc. **172**, 303–318 (1995).
[41]S. Brodersen and B. I. Zhilinskiĭ, J. Mol. Spectrosc. **169**, 1–17 (1995).
[42]J. P. Aldridge, H. Filip, H. Flicker, R. F. Holland, R. S. McDowell, N. G. Nereson, and K. Fox, J. Mol. Spectrosc. **58**, 165–168 (1975).
[43]J. Karczmarek, J. Wright, P. Corkum, and M. Ivanov, Phys. Rev. Lett. **82**, 3420–3423 (1999).
[44]H. S. P. Müller, F. Schlöder, J. Stutzki, and G. Winnewisser, J. Mol. Struct. (THEOCHEM) **742**, 215–227 (2005).
[45]N. Jacquinet-Husson, L. Crepeau, R. Armante, C. Boutammine, A. Chédin, N. A. Scott, C. Crevoisier, V. Capelle, C. Boone, N. Poulet-Crovisier, A. Barbe, A. Campargue, D. C. Benner, Y. Benilan, B. Bézard, V. Boudon, L. R. Brown, L. H. Coudert, A. Coustenis, V. Dana, V. M. Devi, S. Fally, A. Fayt, J.-M. Flaud, A. Goldman, M. Herman, G. J. Harris, D. Jacquemart, A. Jolly, I. Kleiner, A. Kleinböhl, F. Kwabia-Tchana, N. Lavrentieva, N. Lacome, L.-H. Xu, O. M. Lyulin, J.-Y. Mandin, A. Maki, S. Mikhailenko, C. E. Miller, T. Mishina, N. Moazzen-Ahmadi, H. S. P. Müller, A. Nikitin, J. Orphal, V. Perevalov, A. Perrin, D. T. Petkie, A. Predoi-Cross, C. P. Rinsland, J. J. Remedios, M. Rotger, M. A. H. Smith, K. Sung, S. Tashkun, J. Tennyson, R. A. Toth, A.-C. Vandaele, and J. Vander Auwera, J. Quant. Spectrosc. Radiat. Transf. **112**, 2395–2445 (2011).
[46]S. N. Yurchenko, W. Thiel, M. Carvajal, H. Lin, and P. Jensen, Adv. Quantum Chem. **48**, 209–238 (2005).
[47]S. N. Yurchenko, W. Thiel, and P. Jensen, J. Mol. Spectrosc. **245**, 126–140 (2007).
[48]S. N. Yurchenko, R. J. Barber, A. Yachmenev, W. Thiel, P. Jensen, and J. Tennyson, J. Phys. Chem. A **113**, 11845–11855 (2009).
[49]S. N. Yurchenko, R. J. Barber, and J. Tennyson, Mon. Not. R. Astron. Soc. **413**, 1828–1834 (2011).
[50]P. R. Bunker and P. Jensen, in *Molecular Symmetry and Spectroscopy*, 2nd ed. (NRC Research Press, Ottawa, 1998).
[51]P. R. Bunker and P. Jensen, *Fundamentals of Molecular Symmetry* (IOP Publishing, Bristol, 2004).
[52]B. V. Noumerov, Mon. Not. R. Astron. Soc. **84**, 592–602 (1924).
[53]J. W. Cooley, Math. Comput. **15**, 363–374 (1961).
[54]S. N. Yurchenko, M. Carvajalz, P. Jensen, H. Lin, J. J. Zheng, and W. Thiel, Mol. Phys. **103**, 359–378 (2005).
[55]F. S. Pan and T. Oka, Astrophys. J. **305**, 518–525 (1986).
[56]S. Miller, J. Tennyson, B. Follmeg, P. Rosmus, and H. J. Werner, J. Chem. Phys. **89**, 2178–2184 (1988).

[57]W. G. Harter, C. W. Patterson, and F. J. D. Paixao, Rev. Mod. Phys. **50**, 37–83 (1978).
[58]See supplementary material at http://dx.doi.org/10.1063/1.4882865 for a HITRAN-style line list of pure rotational transitions.
[59]J. Tennyson and S. N. Yurchenko, Mon. Not. R. Astron. Soc. **425**, 21–33 (2012).
[60]H. Grosch, A. Fateev, K. L. Nielsen, and S. Clausen, J. Quant. Spectrosc. Radiat. Transf. **130**, 392–399 (2013).
[61]P. R. Bunker and P. Jensen, J. Mol. Spectrosc. **228**, 640–644 (2004).
[62]D. S. Underwood, J. Tennyson, and S. N. Yurchenko, "ExoMol Molecular linelists: X A variationally computed line-list for hot SO_3," Mon. Not. R. Astron. Soc. (unpublished).